A Natural Vanadate–Arsenate Isomorphous Series with Jeffbenite-Type Structure: New Fumarolic Minerals Udinaite, NaMg₄(VO₄)₃, and Arsenudinaite, NaMg₄(AsO₄)₃

Igor V. Pekov [1], Natalia N. Koshlyakova [1,*], Natalia V. Zubkova [1], Dmitry I. Belakovskiy [2], Marina F. Vigasina [1], Atali A. Agakhanov [2], Dmitry A. Ksenofontov [1], Anna G. Turchkova [1], Sergey N. Britvin [3], Evgeny G. Sidorov [4] and Dmitry Yu. Pushcharovsky [1]

[1] Faculty of Geology, Moscow State University, Vorobievy Gory, 119991 Moscow, Russia; igorpekov@mail.ru (I.V.P.); n.v.zubkova@gmail.com (N.V.Z.); vigasina@geol.msu.ru (M.F.V.); ksen53@gmail.com (D.A.K.); annaturchkova@mail.ru (A.G.T.); dmitp@geol.msu.ru (D.Y.P.)

[2] Fersman Mineralogical Museum of the Russian Academy of Sciences, Leninsky Prospekt 18-2, 119071 Moscow, Russia; dmzvr@mail.ru (D.I.B.); atali99@mail.ru (A.A.A.)

[3] Department of Crystallography, St. Petersburg State University, University Emb. 7/9, 199034 St. Petersburg, Russia; sbritvin@gmail.com

[4] Institute of Volcanology and Seismology, Far Eastern Branch of Russian Academy of Sciences, Piip Boulevard 9, 683006 Petropavlovsk-Kamchatsky, Russia; mineral@kscnet.ru

[*] Correspondence: nkoshlyakova@gmail.com

Abstract: Two new isostructural minerals udinaite and arsenudinaite with the end-member formulae NaMg₄(VO₄)₃ and NaMg₄(AsO₄)₃, respectively, are found in the Arsenatnaya fumarole, Tolbachik volcano, Kamchatka, Russia. They are associated with one another and anhydrite, diopside, hematite, schäferite, berzeliite, svabite, calciojohillerite, tilasite, reznitskyite, ludwigite, rhabdoborite-group borates, forsterite, magnesioferrite, fluorapatite, pliniusite, and powellite. Both minerals occur as equant tetragonal prismatic–dipyramidal crystals up to 0.15 mm, aggregates up to 1 cm and interrupted crusts up to 2 × 2 cm². Udinaite and arsenudinaite, visually indistinguishable from one another, are transparent, beige or brownish-yellowish, with vitreous lustre. Both minerals are optically uniaxial (–); ω = 1.785/1.777 and ε = 1.830/1.820, $D_{calc.}$ = 3.613/3.816 g·cm⁻³ (udinaite/arsenudinaite). The empirical formulae are: udinaite: (Na₀.₅₅Ca₀.₁₆)Σ₀.₇₁(Mg₄.₀₄Mn₀.₀₂Fe₀.₀₁)Σ₄.₀₇(V₁.₆₃As₁.₀₅P₀.₂₈Si₀.₀₃S₀.₀₁)Σ₃.₀₀O₁₂; arsenudinaite: (Na₀.₅₇Ca₀.₁₃)Σ₀.₇₀(Mg₄.₀₁Mn₀.₀₁Fe₀.₀₁)Σ₄.₀₃(As₂.₀₇V₀.₈₄P₀.₁₀Si₀.₀₁S₀.₀₁)Σ₃.₀₃O₁₂. Both minerals are tetragonal, $I\text{-}42d$, Z = 4, a = 6.8011(2)/6.8022(1), c = 19.1839(12)/19.1843(6) Å, and V = 887.35(7)/887.66(4) Å³, R_1 = 0.0287/0.0119 (udinaite/arsenudinaite). Their crystal structure consists of the helical chains of edge-sharing MgO₆ octahedra and isolated TO₄ tetrahedra, forming a heteropolyhedral pseudo-framework with Na cations located in cavities. Both minerals are isostructural to jeffbenite. Udinaite and arsenudinaite form an isomorphous series in which the contents of T constituents vary within (in *apfu*): V₁.₆₋₀.₁As₂.₈₋₁.₀P₀.₄₋₀.₀.

Keywords: udinaite; arsenudinaite; new mineral; jeffbenite; TAPP; crystal structure; fumarole sublimate; Tolbachik volcano; Kamchatka

1. Introduction

In this paper, we describe two new minerals: udinaite (Cyrillic: удинаит), ideally NaMg₄(VO₄)₃, and arsenudinaite (Cyrillic: арсенудинаит), ideally NaMg₄(AsO₄)₃. They are isostructural and form a solid-solution series in which the major variable is the V⁵⁺:As⁵⁺ ratio. Synthetic analogues of both vanadate and arsenate end members of this series were earlier known; however, the intermediate members were not synthesized, and thus, the isomorphous series is novel.

Udinaite is named after the Udina volcano situated near the discovery locality. The picturesque Udina volcanic massif consists of two extinct conical stratovolcanoes, Bol'shaya

Udina (2920 m) and Malaya Udina (1945 m). Arsenudinaite is named as an analogue of udinaite with As > V. Both new minerals and their names have been approved by the IMA Commission on New Minerals, Nomenclature and Classification: IMA2018–066 (udinaite) and IMA2018–067 (arsenudinaite). The type specimens are deposited in the systematic collection of the Fersman Mineralogical Museum of the Russian Academy of Sciences, Moscow, with the catalogue numbers 96,272 (udinaite) and 96,273 (arsenudinaite).

2. Occurrence and Mineral Associations

Minerals of the udinaite–arsenudinaite series were found in the Arsenatnaya fumarole located at the Second scoria cone of the Northern Breakthrough of the Great Tolbachik Fissure Eruption 1975–1976, Tolbachik volcano, Kamchatka Peninsula, Far-Eastern Region, Russia (55°41′ N 160°14′ E, 1200 m asl). This scoria cone is a monogenetic volcano about 300 m high and ca. 0.1 km^3 in volume, formed in 1975 [1]. Strong fumarolic activity occurs here currently. The active, hot Arsenatnaya fumarole belonging to the oxidizing type is characterized by an outstanding mineral diversity and uniqueness. Arsenatnaya, first uncovered by us in 2012, already became a famous mineral locality in which 62 new IMA-approved mineral species were discovered. This fumarole, its general mineralogical features and zonation pattern are described in [2,3].

The type specimens of both udinaite and arsenudinaite were collected by us in July 2016 from deep (3–4 m) under the day surface, the hottest zone of the Arsenatnaya fumarole. The temperatures in this area measured, using a chromel–alumel thermocouple, during collecting were 450–470 °C. Sublimate incrustations in this zone are up to 4 cm thick and usually mainly consist of anhydrite, diopside and hematite, typically with significant amounts of arsenate–vanadate garnets of the berzeliite–schäferite series and svabite. Udinaite and arsenudinaite are associated, besides these minerals, with one another and with calciojohillerite, tilasite, reznitskyite, ludwigite, rhabdoborite-group borates, forsterite, magnesioferrite, fluorapatite, pliniusite, arsenowagnerite, wagnerite, powellite, scheelite, and baryte.

In July 2021 in the upper part of this zone, the As-richest variety of arsenudinaite close to the end-member $NaMg_4(AsO_4)_3$ was found. It is associated with hematite, fluorophlogopite, sanidine, forsterite, enstatite, calciojohillerite, and fluorapatite–svabite series members.

3. Methods

The Raman spectrum of As-rich udinaite was obtained using an EnSpectr R532 spectrophotometer (Department of Mineralogy, Moscow State University, Moscow, Russia) with a green laser (532 nm) at room temperature. The output power of the laser beam on the sample was about 7 mW. The spectrum was processed in the range from 100 to 4000 cm^{-1} with the use of a holographic diffraction grating with 1800 mm^{-1} and a resolution equal to 6 cm^{-1}. The diameter of the focal spot on the sample was about 10 μm with 40× objective. The spectrum was acquired on a crystal cluster.

Scanning electron microscopic (SEM) studies in secondary electron (SE) mode were carried out, and chemical composition was determined for all studied samples using a JEOL JSM-6480LV scanning electron microscope equipped with an INCA-Wave 500 wavelength-dispersive spectrometer (Laboratory of Analytical Techniques of High Spatial Resolution, Department of Petrology, Moscow State University, Moscow, Russia), with an acceleration voltage of 20 kV, a beam current of 20 nA, and a 5 μm beam diameter. The standards used are as follows: Na (jadeite), K ($KTiOPO_4$), Ca ($CaSiO_3$), Pb (PbTe), Mg (diopside), Mn (Mn), Cu ($CuFeS_2$), Zn (ZnS), Sr ($SrSO_4$), Fe (FeS_2), Si (jadeite), P ($KTiOPO_4$), V (V), As (GaAs), S (ZnS). Contents of other elements with atomic numbers higher than that of carbon are below detection limits.

Powder X-ray diffraction (XRD) data were collected using a Rigaku RAXIS Rapid II diffractometer with curved image plate detector (Department of Crystallography, St. Petersburg State University, St. Petersburg, Russia), rotating anode with VariMAX microfocus optics, using Co$K\alpha$ radiation, in Debye–Scherrer geometry, at accelerating voltage of 40 kV,

current of 15 mA and exposure time at 12 min for each sample. The distance between sample and detector was 127.4 mm. The data were processed using osc2xrd software (Department of Crystallography, St. Petersburg State University, St. Petersburg, Russia) [4].

Single-crystal XRD studies were carried out using an Xcalibur S diffractometer equipped with CCD detector (Mo*K*α radiation) (Department of Crystallography, Moscow State University, Moscow, Russia).

4. Results

4.1. General Appearance and Physical Properties

In the type specimens, udinaite and arsenudinaite, visually indistinguishable from one another, form nearly equant tetragonal crystals up to 0.15 mm across, separate or combined in chains up to 0.5 mm long. The crystals are prismatic–dipyramidal, sometimes pseudo-cuboctahedral, regular or, more commonly, distorted (Figure 1). On them, faces of the pinacoid {001} and the tetragonal prisms {100} and {110} are undoubtedly identified; non-indexed forms include two tetragonal dipyramids {*h0l*} (typically, one of them is the major form: Figure 1a,b), one tetragonal tetrahedron {*hhl*} and one tetragonal scalenohedron {*hkl*} (rare and minor forms). Many crystals are skeletal, case-like and contain anhydrite in the core (Figures 1e and 2). Interesting double epitactic intergrowths were observed: "ribbed" parallel aggregates of small, flattened forsterite crystals epitactically overgrow a larger prismatic anhydrite crystal and crystals of udinaite or arsenudinaite epitactically overgrow forsterite (Figure 1a–c). Both udinaite and arsenudinaite occur as open-work, typically bush-like aggregates up to 1 cm across, in which these minerals are always intimately intergrown with anhydrite. Such aggregates overgrow a surface of anhydrite crusts or are embedded in them together with garnets of the berzeliite–schäferite series, calciojohillerite, rhabdoborite-group borates, and tilasite (Figures 2 and 3). Interrupted crusts consisting of aggregates of udinaite, arsenudinaite and anhydrite cover areas up to 2 cm × 2 cm.

(**a**)   (**b**)

(**c**)

Figure 1. *Cont.*

(**d**)　　　　　　　　　　　　　　　　(**e**)
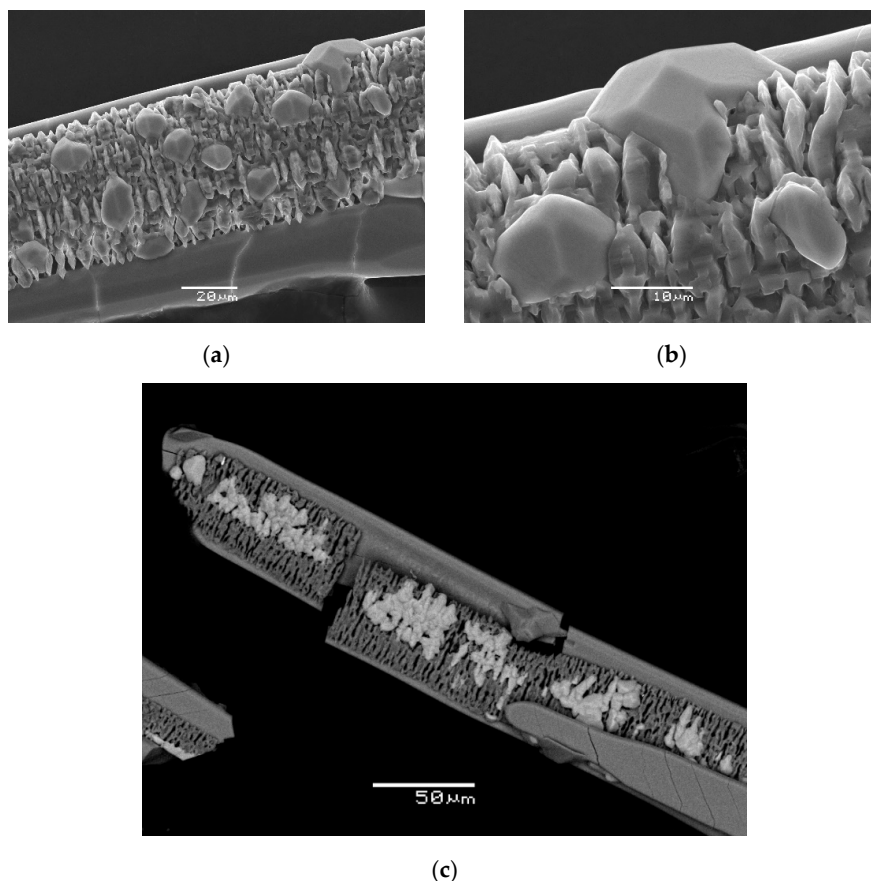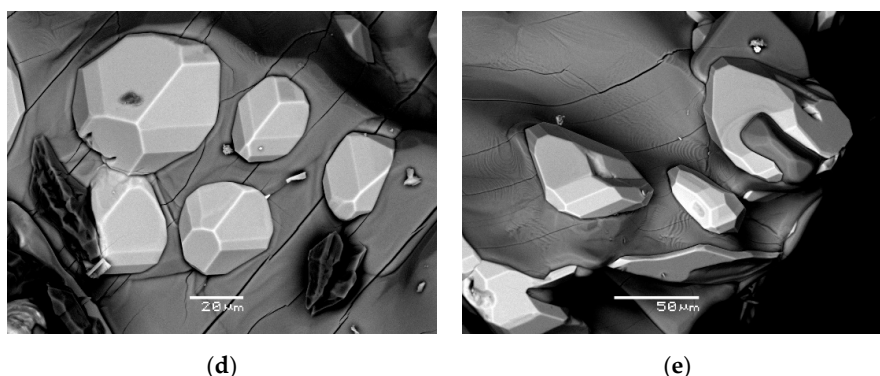
Figure 1. Morphology of crystals and aggregates of holotype udinaite and arsenudinaite: (**a**–**c**) complex epitactic intergrowths: "ribbed" parallel aggregates of small flattened forsterite crystals epitactically overgrow large prismatic anhydrite crystal and pseudo-cuboctahedral crystals of udinaite ((**a**,**b**): (**a**) general view, (**b**) magnified fragment with the largest udinaite crystal) and arsenudinaite (**c**) epitactically overgrow forsterite; (**d**,**e**) well-formed 9almost regular in shape (**d**) and significantly distorted (**e**)) crystals of arsenudinaite (light grey) partially ingrown in surface zone of large anhydrite (grey) crystals. SEM image, SE (**a**,**b**) and BSE (**c**,**e**) modes.
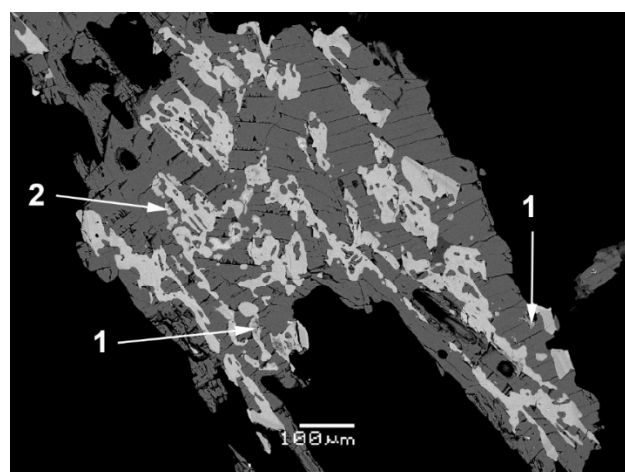
Figure 2. Abundant skeletal, case-like coarse crystals of udinaite (light grey) embedded in anhydrite (dark grey matrix), with small grains of rhabdoborite-(V) (1) and tilasite (2). Polished section, SEM (BSE) image.

The As-richest variety of arsenudinaite found in another association forms coarse short-prismatic crystals up to 0.5 mm × 1 mm, separate or combined in clusters up to 3 mm across overgrowing hematite crystal crusts which cover the surface of basalt scoria altered to sanidine aggregate by fumarolic gas.

Both new minerals are transparent, with vitreous lustre and white streak. They are beige, pale brownish, brownish-yellowish or greyish-brownish; the smallest crystals are almost colourless; the As-richest variety of arsenudinaite is light yellow. Both minerals are brittle. The Mohs' hardness is ca. $3\frac{1}{2}$. Cleavage or parting was not observed, the fracture was uneven. Density was not measured because solid crystals of udinaite and arsenudinaite are small, and the minerals form intimate intergrowths with anhydrite. The density values calculated using the averaged empirical formulae of the holotypes are 3.613 g cm^{-3} for udinaite and 3.816 g cm^{-3} for arsenudinaite.

(**a**)

(**b**)

Figure 3. Aggregates of beige udinaite (**a**) and arsenudinaite (**b**) intimately associated with colourless to bluish prismatic anhydrite, yellow-orange garnets of the berzeliite–schäferite series and minor black hematite. FOV width: (**a**) 8.8 mm, (**b**) 11.4 mm. Photo: I.V. Pekov and A.V. Kasatkin.

4.2. Optical Data

In plane-polarized transmitted light, udinaite and arsenudinaite are colourless and non-pleochroic. Both minerals are optically uniaxial (–). The refractive indices are given in Table 1.

Table 1. Comparative data for udinaite and arsenudinaite.

Mineral	Udinaite	Arsenudinaite
Ideal, end-member formula	$NaMg_4(VO_4)_3$	$NaMg_4(AsO_4)_3$
Crystal system	Tetragonal	
Space group	*I*-42*d*	
a, Å	6.8011 (2)	6.8022 (1)
c, Å	19.1839 (12)	19.1843 (6)
V, Å³	887.35 (7)	887.66 (4)
Z	4	4
$D_{calc.}$, g cm^{-3}	3.613	3.816
Strongest reflections of the powder X-ray diffraction pattern:*d*, Å—*I*	4.654–19	4.657–26
	4.294–22	4.300–24
	3.340–28	3.341–29
	3.003–48	3.007–46
	2.774–100	2.775–100
	2.747–17	2.750–17
	2.663–16	2.663–17
	1.699–26	1.698–27
Optical data	Uniaxial (–)	Uniaxial (–)
ω	1.785 (8)	1.777 (10)
ε	1.830 (6)	1.820 (6)

4.3. Raman Spectroscopy

The Raman spectrum of As-rich udinaite (holotype, Figure 4) was interpreted according to [5]. The bands in the region 750–950 cm^{-1} correspond to V^{5+}–O and As^{5+}–O stretching vibrations of tetrahedral VO$_4$ and AsO$_4$ groups. Bands with frequencies lower than 500 cm^{-1} correspond to V^{5+}–O and As^{5+}–O bending vibrations of VO_4^{3-} and AsO_4^{3-} anions, Mg–O stretching vibrations and lattice modes. The absence of bands with frequencies higher than 950 cm^{-1} indicates the absence of groups with O–H, C–H, C–O, N–H, N–O and B–O bonds in udinaite.
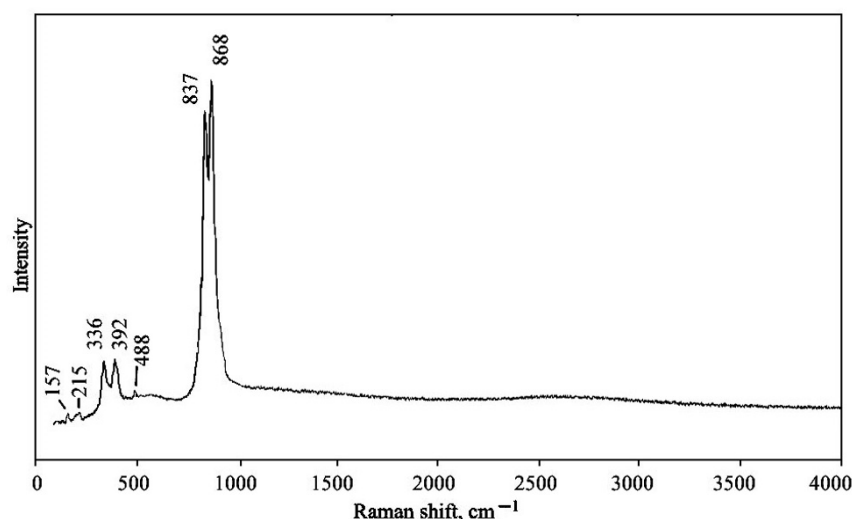
Figure 4. The Raman spectrum of the holotype udinaite.

4.4. Chemical Data

Chemical composition of udinaite and arsenudinaite are given in Table 2 (representative analyses sorted by descending of V$_2$O$_5$ content). The empirical formulae were calculated on the basis of 12 O atoms per formula unit (*apfu*).

Table 2. Chemical composition of udinaite–arsenudinaite series minerals.

No.	1 *	2	3	4	5	6	7	8	9	10 *	11	12	13 *
Mineral	Udn (ht)	Udn	Udn	Udn	Udn	AsUdn	AsUdn	AsUdn	AsUdn	AsUdn (ht)	AsUdn	AsUdn	AsUdn
						wt. %							
Na_2O	3.51 (3.37–3.63)	3.63	3.00	3.57	4.08	3.67	3.63	2.86	3.59	3.43 (3.18–3.89)	3.18	3.04	6.11
K_2O					0.01			0.01				0.01	
CaO	1.8 (1.69–1.94)	1.76	1.62	1.54	2.27	1.45	1.53	1.62	1.04	1.41 (0.93–2.40)	2.40	0.98	
SrO		0.35		0.24		0.05							
PbO	0.14 (0.00–0.36)												
MgO	33.54 (32.51–34.16)	32.51	33.48	32.84	33.12	32.52	31.82	31.40	31.17	31.48 (30.61–32.56)	31.40	30.61	30.04
MnO	0.29 (0.25–0.37)	0.25	0.26	0.20	0.42	0.21	0.16	0.10	0.26	0.17 (0.10–0.26)	0.17	0.14	
CuO	0.03 (0.00–0.08)	0.08	0.05	0.10	0.15	0.09		0.05	0.03	0.03 (0.00–0.06)		0.01	
ZnO			0.01		0.02								
Fe_2O_3	0.21 (0.18–0.27)	0.20	0.10	0.13	0.31	0.10	0.21	0.04	0.23	0.09 (0.00–0.23)		0.04	
SiO_2	0.38 (0.22–0.65)	0.22	0.14	0.24	0.95	0.26	0.07	0.09	0.06	0.1 (0.06–0.21)	0.07	0.21	
P_2O_5	4.11 (3.59–4.82)	4.08	2.75	3.42	5.38	3.70	1.83	0.47	2.20	1.33 (0.22–2.33)	2.03	0.22	1.10
V_2O_5	30.51 (29.25–31.14)	30.13	28.12	25.80	24.11	22.37	22.26	18.83	15.01	14.82 (11.47–18.83)	13.01	12.56	1.55
As_2O_5	24.75 (24.07–25.60)	25.60	31.41	31.74	28.22	35.00	36.95	44.06	45.26	46.34 (43.67–50.61)	46.50	50.61	60.53
SO_3	0.22 (0.21–0.24)	0.22	0.03	0.18	0.16	0.14	0.16	0.18	0.07	0.14 (0.07–0.28)	0.09	0.13	
Total	99.49	99.03	100.97	100.0	99.20	99.56	98.62	99.71	98.92	99.34	98.85	98.56	99.33
					Formula calculated on the basis of 12 O atoms per formula unit								
Na	0.55	0.57	0.47	0.57	0.65	0.59	0.59	0.47	0.59	0.57	0.53	0.51	1.05
Ca	0.16	0.15	0.14	0.13	0.20	0.13	0.14	0.15	0.09	0.13	0.22	0.09	
Sr		0.02		0.01		0.02							
Mg	4.04	3.95	4.03	4.00	4.03	4.00	4.00	3.97	3.97	4.01	4.03	3.98	3.99
Mn	0.02	0.02	0.02	0.01	0.03	0.01	0.01	0.01	0.02	0.01	0.01	0.01	
Cu	-	0.01	-	0.01	0.01	0.01		-	-	-		-	
Fe	0.01	0.01	0.01	0.01	0.02	0.01	0.01	-	0.01	0.01		-	
Si	0.03	0.02	0.01	0.02	0.08	0.02	0.01	0.01	0.01	0.01	0.01	0.02	
P	0.28	0.28	0.19	0.24	0.37	0.26	0.13	0.03	0.16	0.10	0.15	0.02	0.08
V	1.63	1.62	1.50	1.39	1.30	1.22	1.24	1.05	0.85	0.84	0.74	0.72	0.09
As	1.05	1.09	1.33	1.36	1.20	1.51	1.63	1.95	2.02	2.07	2.09	2.31	2.82
S	0.01	0.01	-	0.01	0.01	0.01	0.01	0.01	-	0.01	0.01	0.01	
ΣA	I	0.74	0.61	0.71	0.85	0.74	0.73	0.62	0.68	0.70	0.75	0.60	1.05
ΣM	4.07	3.99	4.06	4.03	4.09	4.03	4.02	3.98	4.00	4.03	4.04	3.99	3.99
ΣT	3.00	3.02	3.03	3.02	2.96	3.02	3.02	3.05	3.04	3.03	3.00	3.08	2.99

ΣA = Na + Ca + Sr; ΣM = Mg + Mn + Cu + Fe; ΣT = As + V + P + Si + S; empty cell means the content was below detection limit, and dash means 0.00 apfu (for minor admixtures). Udn—udinaite, AsUdn—arsenudinaite; (ht)—composition of holotype specimens (averaged on 6 analyses each), ranges are in parentheses. *Analyses 1, 10 and 13 correspond to samples *(1)*, *(2)* and *(3)*, respectively, with studied crystal structure (see below).

These data, together with Figure 5, demonstrate that the new minerals form an iso-morphous series with the As:V ratio as the major variable: V_2O_5 content varies from 31.1 to 1.5 wt.% and As_2O_5 content from 24.1 to 60.5 wt.%. The third significant variable is P, from 0.2 to 5.4 wt.% P_2O_5 (Table 2). Thus, the composition of minerals of the udinaite–arsenudinaite series changes mainly due to the homovalent substitutions at the tetrahedral

position *T* (for structure data see below): $As^{5+} \leftrightarrow V^{5+} (\leftrightarrow P^{5+})$. The contents of tetrahedrally coordinated constituents vary in the following limits (in *apfu*): $V_{1.6–0.1}As_{2.8–1.0}P_{0.4–0.0}$. Admixtures of other *T* constituents are insignificant (*apfu*): 0.00–0.08 Si and 0.00–0.01 S (Table 2). Slight positive correlation between V and P contents is observed (Figure 5).
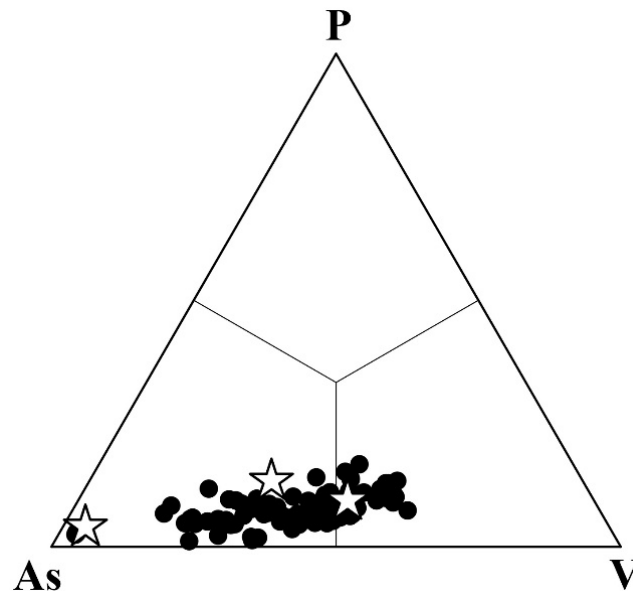
Figure 5. Ratios of major tetrahedrally coordinated constituents (*T*) in minerals of the udinaite–arsenudinaite isomorphous series. Compositions of single crystals with studied crystal structures are given as white stars.

The octahedrally coordinated position *M* is almost fully occupied by Mg in all studied samples; the contents of admixtures (Fe, Mn, Cu and Zn) is insignificant: not higher than 0.06 *apfu* together (Table 2).

The large-cation position *A* is predominantly occupied by Na, typically with Ca admixture (up to 0.22 *apfu*), and is usually partially vacant: the cation deficiency reaches 0.39 apfu (#4 in Table 2). It is not excluded that minor admixture of Mn is also in the *A* site.

The empirical formulae of the holotype specimens (averaged on six analyses each) are: udinaite (#1 in Table 2):

$(Na_{0.55}Ca_{0.16})_{\Sigma0.71}(Mg_{4.04}Mn_{0.02}Fe_{0.01})_{\Sigma4.07}(V_{1.63}As_{1.05}P_{0.28}Si_{0.03}S_{0.01})_{\Sigma3.00}O_{12}$;
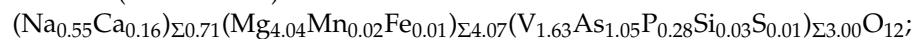
arsenudinaite (#10 in Table 2):

$(Na_{0.57}Ca_{0.13})_{\Sigma0.70}(Mg_{4.01}Mn_{0.01}Fe_{0.01})_{\Sigma4.03}(As_{2.07}V_{0.84}P_{0.10}Si_{0.01}S_{0.01})_{\Sigma3.03}O_{12}$.
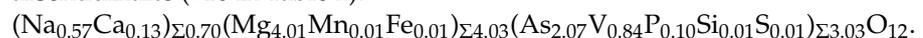
The simplified, end-member formula of arsenudinaite is $NaMg_4(AsO_4)_3$, and of udinaite is $NaMg_4(VO_4)_3$, which requires Na_2O 5.77, MgO 30.02, As_2O_5 64.21, total 100 wt% for arsenudianite and Na_2O 6.66, MgO 34.67, V_2O_5 58.67, total 100 wt% for udinaite.

4.5. X-ray Crystallography and Crystal Structure

Powder XRD data of both holotype udinaite and arsenudinaite are given in Table 3. The unit-cell parameters calculated from the powder data are as follows: udinaite: *a* = 6.806(1), *c* = 19.196(9) Å, and *V* = 889.2(7) Å³; arsenudinaite: *a* = 6.808(1), *c* = 19.186(9) Å, and *V* = 889.1(6) Å³.

Crystal structures were studied for three single crystals with different As:V ratios: holotype specimens of udinaite *(1)* and arsenudinaite *(2)* and a sample of the As-richest arsenudinaite chemically close to the end-member formula *(3)* (##1, 10 and 13, respectively, in Table 2).

Table 3. Powder X-ray diffraction data (d in Å) of udinaite and arsenudinaite.

Udinaite				Arsenudinaite				hkl
I_{meas}	d_{meas}	I_{calc} *	d_{calc} **	I_{meas}	d_{meas}	I_{calc} *	d_{calc} **	
1	6.406	1	6.410			1	6.441	101
7	4.792	5	4.796	9	4.792	5	4.796	004
19	4.654	16	4.659	26	4.657	16	4.659	103
22	4.294	15	4.299	24	4.300	17	4.300	112
28	3.340	23	3.342	29	3.341	23	3.342	105
7	3.204	6	3.205	9	3.208	6	3.206	202
48	3.003	40	3.004	46	3.007	40	3.005	211
100	2.774	100	2.774	100	2.775	100	2.774	204
17	2.747	14	2.747	17	2.750	14	2.747	213
16	2.663	14	2.663	17	2.663	14	2.663	116
10	2.400	3	2.405	8	2.399	4	2.405	220
		9	2.398			9	2.398	008
		2	2.383	4	2.387	2	2.384	215
11	2.328	8	2.329	12	2.330	7	2.330	206
3	2.037	3	2.036	4	2.037	3	2.036	217
3	1.962	3	1.962	3	1.963	3	1.963	314
10	1.878	7	1.877	5	1.874	7	1.878	321
5	1.810	4	1.809	4	1.811	4	1.809	323
4	1.784	3	1.785	4	1.784	3	1.785	316
		2	1.782			2	1.782	1.1.10
9	1.749	2	1.747	8	1.749	2	1.747	307
		8	1.746			8	1.746	219
26	1.699	15	1.700	27	1.698	15	1.701	400
		23	1.698			23	1.698	228
		13	1.693			13	1.693	325
1	1.675	2	1.674	2	1.676	2	1.674	402
6	1.599	3	1.601	6	1.599	3	1.601	318
		1	1.599			1	1.599	0.0.12
		2	1.597			2	1.597	413
9	1.555	6	1.554	8	1.555	6	1.554	327
		6	1.553			6	1.553	309
7	1.524	3	1.521	7	1.525	3	1.521	420
9	1.517	7	1.515	8	1.517	7	1.516	415
4	1.503	2	1.502	4	1.503	2	1.502	422
		2	1.501			3	1.501	406
10	1.450	10	1.450	10	1.449	10	1.450	424
		9	1.447			10	1.447	2.0.12
5	1.433	3	1.433	5	1.434	4	1.433	336
		3	1.432			3	1.432	3.1.10
2	1.389	4	1.387	2	1.388	4	1.387	408
3	1.375	5	1.373	3	1.375	5	1.374	426
3	1.358	3	1.357	2	1.359	4	1.357	501
3	1.334	4	1.334	2	1.334	4	1.334	510

* For the calculated patterns, only reflections with intensities ≥ 1 are given; ** the unit-cell parameters calculated from single-crystal data. The strongest reflections are marked in bold type.

The crystal structures were solved by direct methods with the SHELX software package [6] and refined to:

R_1 = 0.0287 for 544 independent reflections with I > 2σ(I) *(1)*;
R_1 = 0.0119 for 554 independent reflections with I > 2σ(I) *(2)*;
R_1 = 0.0151 for 543 independent reflections with I > 2σ(I) *(3)*.

Crystal data, data collection information and structure refinement details are given in Table 4, atom coordinates and displacement parameters are in Table 5, and selected interatomic distances in Table 6.

Table 4. Crystal data, data collection information and structure refinement details for udinaite and two chemical varieties of arsenudinaite.

Sample	*(1)* **Holotype Udinaite**	**(2) Holotype Arsenudinaite**	**(3) As-Richest Arsenudinaite**
Crystal chemical formula	$(Na_{0.70}Ca_{0.15})_{\Sigma 0.85}$ Mg_4 $(V_{1.35}As_{1.33}P_{0.32})_{\Sigma 3.00}O_{12}$	$(Na_{0.70}Ca_{0.15})_{\Sigma 0.85}$ Mg_4 $(As_{1.64}V_{0.96}P_{0.40})_{\Sigma 3.00}O_{12}$	Na Mg_4 $(As_{2.76}V_{0.12}P_{0.12})_{\Sigma 3.00}O_{12}$
Formula weight	489.67	495.38	528.84
Crystal system, space group, Z	Tetragonal, *I*-42*d*, 4		
a, Å	6.8011 (2)	6.8022 (1)	6.79122(12)
c, Å	19.1839 (12)	19.1843 (6)	19.1590(6)
V, Å³	887.35 (7)	887.66 (4)	883.63(4)
F(000)	938	947	1003
μ (mm⁻¹)	6.923	7.684	10.94
Absorption correction	gaussian		
Crystal dimensions (mm)	0.06 × 0.08 × 0.10	0.08 × 0.13 × 0.16	0.15 × 0.21 × 0.32
Diffractometer	Xcalibur S CCD		
Temperature (K)	293		
Radiation	Mo*K*α, λ = 0.71073 Å		
θ range (°)	3.18–32.13	3.18–28.28	4.25–29.92
Range of *h*, *k*, *l*	−9 → 9, −9 → 9, −25 → 25	−9 → 9, −9 → 9, −25 → 25	−9 → 9, −9 → 9, −25 → 25
Numbers of measured, independent and observed [*I* > 2σ(*I*)] reflections	7155, 552, 544	6977, 557, 554	6193, 546, 543
R_{int}	0.0815	0.0359	0.0469
Structure solution	direct methods		
Refinement on	F^2		
*R*1 and *wR*2 for *I* > 2σ(*I*)	0.0287, 0.0614	0.0119, 0.0348	0.0151, 0.0430
*R*1 and *wR*2 for all data	0.0295, 0.0617	0.0118, 0.0348	0.0152, 0.0430
Number of parameters refined	49	49	47
$\Delta\rho_{max}$, $\Delta\rho_{min}$ (e Å⁻³)	0.545, −0.713	0.217, −0.510	0.267, −0.443
GooF	1.160	1.281	1.209
Weighting scheme	w = 1/[σ²($F_o{}^2$) + (0.0250P)² + 2.2343P]	w = 1/[σ²($F_o{}^2$) + (0.0153P)² + 0.8144P] p = ([max of (0 or $F_o{}^2$)] + 2Fc^2)/3	w = 1/[σ²($F_o{}^2$) + (0.0175P)² + 2.2732P]

Table 5. Coordinates and equivalent displacement parameters (U_{eq}, in Å^2) of atoms, site occupancy factors (s.o.f.) and site multiplicities (Q) for holotype udinaite (1), holotype arsenudinaite (2), and the As-richest arsenudinaite (3).

Site	№	x	y	z	U_{eq}	s.o.f.	Q
$T(1)$	(1)				0.0078(2)	$As_{0.60}V_{0.28}P'_{0.12}$	
	(2)	0	0	0	0.00643(12)	$As_{0.72}V_{0.12}P'_{0.16}$	4
	(3)				0.0046(2)	$As_{0.92}V_{0.04}P'_{0.04}$	
$T(2)$	(1)	0.34580(12)			0.00720(19)	$V_{0.57}As_{0.35}P'_{0.08}$	
	(2)	0.34557(6)	0.25	0.125	0.00550(10)	$As_{0.46}V_{0.42}P'_{0.12}$	8
	(3)	0.34481(10)			0.00697(17)	$As_{0.92}V_{0.04}P'_{0.04}$	
$M(1)$	(1)			0.02167(10)	0.0117(4)		
	(2)	0	0.5	0.02167(5)	0.0102(2)	$Mg_{1.00}$	8
	(3)			0.02064(10)	0.0066(4)		
$M(2)$	(1)	0.7598(3)			0.0114(4)		
	(2)	0.75977(17)	0.25	0.125	0.0090(2)	$Mg_{1.00}$	8
	(3)	0.7591(3)			0.0072(4)		
A	(1)				0.0172(8)	$Na_{0.70}Ca_{0.15}\square_{0.15}$	
	(2)	0	0	0.5	0.0163(4)	$Na_{0.70}Ca_{0.15}\square_{0.15}$	4
	(3)				0.0126(8)	$Na_{1.00}$	
O(1)	(1)	0.5056(5)	0.2032(4)	0.05940(14)	0.0118(6)		
	(2)	0.5060(3)	0.2033(2)	0.05939(8)	0.0114(3)	$O_{1.00}$	16
	(3)	0.5058(5)	0.2055(5)	0.05960(15)	0.0085(7)		
O(2)	(1)	0.2250(5)	0.4544(4)	0.09941(15)	0.0142(7)		
	(2)	0.2247(3)	0.4544(2)	0.09947(8)	0.0123(3)	$O_{1.00}$	16
	(3)	0.2234(5)	0.4529(4)	0.10007(15)	0.0090(6)		
O(3)	(1)	0.9439(4)	0.2034(4)	0.04413(15)	0.0119(7)		
	(2)	0.9440(2)	0.2047(2)	0.04406(8)	0.0114(3)	$O_{1.00}$	16
	(3)	0.9418(5)	0.2054(5)	0.04375(16)	0.0082(6)		

Admixtures of Si and S which were considered together with P and signed as P'.

Table 6. Selected interatomic distances (Å) in the structures of holotype udinaite *(1)*, holotype arsenudinaite *(2)*, and arsenudinaite close to ideal end-member formula *(3)*.

	(1) **Holotype Udinaite**	*(2)* **Holotype Arsenudinaite**	*(3)* **As-Richest Arsenudinaite**
$T(1)$–O(3)	1.666(3) × 4	1.6727(16) × 4	1.6749(31) × 4
<$T(1)$–O>	1.666	1.673	1.675
$T(2)$–O(2)	1.688(3) × 2	1.6877(16) × 2	1.6753(30) × 2
−O(1)	1.693(3) × 2	1.6961(16) × 2	1.6901(31) × 2
<$T(2)$–O>	1.691	1.692	1.683
$M(1)$–O(1)	2.081(3) × 2	2.0814(17) × 2	2.0765(32) × 2
−O(3)	2.098(3) × 2	2.0894(17) × 2	2.0867(31) × 2
−O(2)	2.159(3) × 2	2.1588(17) × 2	2.1725(32) × 2
<$M(1)$–O>	2.113	2.110	2.112
$M(2)$–O(3)	2.018(3) × 2	2.0189(18) × 2	2.0136(34) × 2
−O(2)	2.072(3) × 2	2.0724(16) × 2	2.0770(30) × 2
−O(1)	2.162(4) × 2	2.1596(19) × 2	2.1495(38) × 2
<$M(2)$–O>	2.084	2.084	2.080
A–O(1)	2.318(3) × 4	2.3182(17) × 4	2.3035(31) × 4
−O(2)	2.689(3) × 4	2.6917(17) × 4	2.7032(32) × 4

5. Discussion

5.1. Structure Description

Udinaite and arsenudinaite are isostructural to one another and to their synthetic end-member analogues, $NaMg_4(VO_4)_3$ [7] and $NaMg_4(AsO_4)_3$ [8], respectively. Their crystal structure (Figure 6) is based on the helical chains of edge-sharing octahedra MO_6 (M = Mg) running along [100] and [010]. The perpendicular chains are linked via common O vertices. The structure contains two crystallographically non-equivalent tetrahedral sites $T(1)$ and $T(2)$ (species-defining $T = V^{5+}$, As^{5+}). Adjacent parallel chains of octahedra MO_6 are connected via $T(2)O_4$ tetrahedra, which share two vertices with octahedra of one chain and an edge with octahedra of the neighbouring parallel chain (Figure 7a). Each $T(1)O_4$ tetrahedron shares all vertices with octahedra MO_6—two with octahedra of one chain and two with octahedra of the perpendicular chain. As a result, a heteropolyhedral M-T-O pseudo-framework is formed. Large cations A (Na with admixed Ca) are located in cavities of the pseudo-framework and centre eight-fold polyhedra with four short A–O distances and four elongated ones (Table 6; Figure 7b). The A sites are partially vacant; this feature is also typical for many synthetic representatives of the $NaMg_4(VO_4)_3$ structure type (here and below, $\square$ means vacancy): $^{VIII}(Mg_{0.5}\square_{0.5})^{VI}Mg_4{}^{IV}As_3O_{12}$ [9], $^{VIII}(Co_{0.5}\square_{0.5})^{VI}Co_4{}^{IV}As_3O_{12}$ [10], $^{VIII}(\square_{0.65}Ni_{0.35})^{VI}Ni_4{}^{IV}As_3O_{11.70}(OH)_{0.30}$ [11], $^{VIII}(Mg_{0.52}Fe^{3+}{}_{0.33}\square_{0.15})^{VI}(Fe^{3+}{}_{2.40}Mg_{1.60})^{IV}(Ge_{2.56}Fe^{3+}{}_{0.44})O_{12}$, $^{VIII}(Y_{0.68}Mg_{0.21}\square_{0.11})^{VI}(Fe^{3+}{}_{2.45}Mg_{1.55})^{IV}(Ge_{2.08}Fe^{3+}{}_{0.92})O_{12}$ [12], $^{VIII}(Mn^{2+}{}_{0.5}\square_{0.5})^{VI}Mn^{2+}{}_4{}^{IV}V_3O_{12}$ [13].
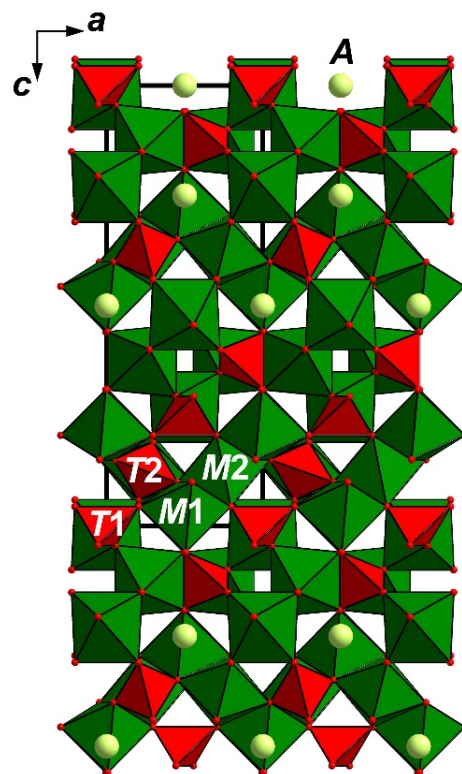
Figure 6. The crystal structure of udinaite/arsenudinaite: T = (As, V)- and (V, As)-centred tetrahedra, M = Mg-centred octahedra and A = (Na, Ca) cations (for details, see also Table 5). The unit cell is outlined.
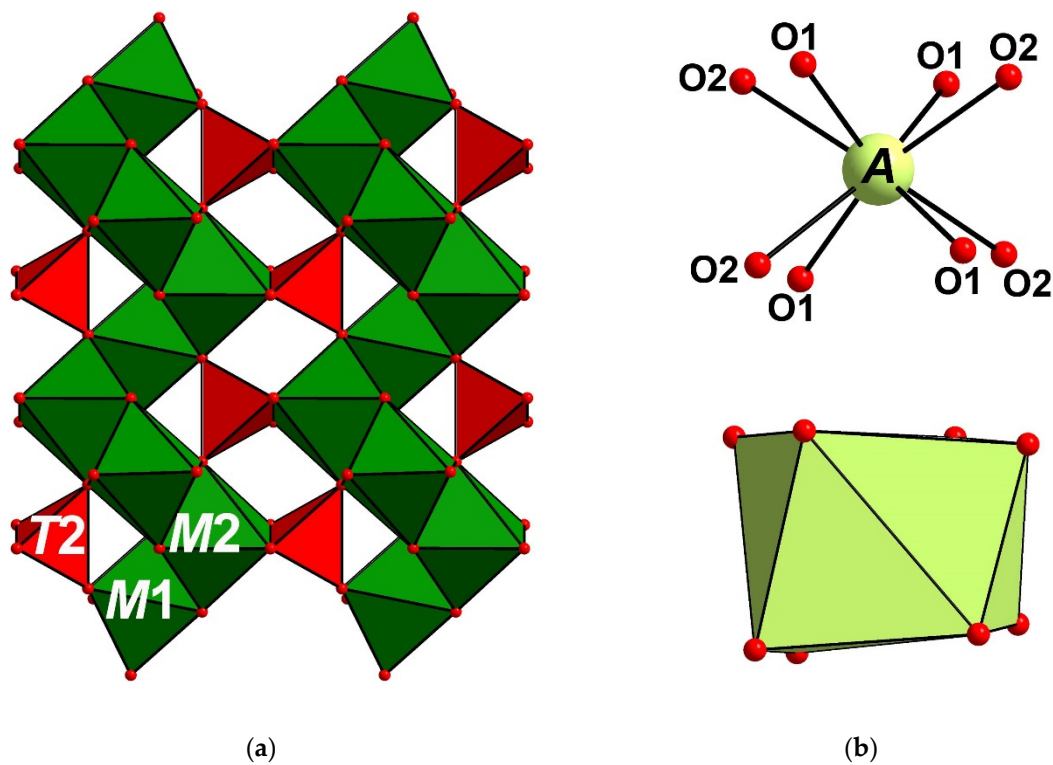
Figure 7. Two parallel helical chains of MO_6 octahedra connected via $T(2)O_4$ tetrahedra (**a**) and coordination environment and coordination polyhedron of the A cation (**b**) in the structure of udinaite/arsenudinaite. For legend, see Table 5.

Udinaite and arsenudinaite differ from one another mainly in occupancies of the tetrahedrally coordinated *T* sites (Table 2).

The distribution of constituents between the *T*(1) and *T*(2) sites in the holotype crystals *(1)* and *(2)* was evaluated on the basis of the refined numbers of electrons; in both cases, As vs. V were refined. As the electron microprobe data show, all crystals contain only admixtures of Si and S, which were considered together with P and signed as *P′* in Table 5. Close *T*(1)-O and *T*(2)-O distances allow one to assume that admixtures *P′* are distributed between *T*(1) and *T*(2) approximately equally or with insignificant preference to *T*(1) due to slightly shorter *T*(1)-O distances in comparison with *T*(2)-O (Table 6). For holotype udinaite and arsenudinaite, *P′* admixture was added in both *T* sites, and the corresponding occupancies for the *T* sites were fixed during the refinement. The refinement of As vs. V gave the following refined numbers of electrons (e_{ref}): 28.1 for *T*(1) and 25.9 for *T*(2) in holotype udinaite and 28.9 for *T*(1) and 26.7 for *T*2 in holotype arsenudinaite. In both studied crystals, the *T*(1) site is As-dominant while the *T*(2) site is V-dominant in udinaite and As-dominant in arsenudinaite. Arsenudinaite *(3)* has low contents of both V and P, and As strongly prevails in both *T*-sites; thus, for the crystal *(3)*, the occupancies of both these admixtures were fixed during the refinement.

We assume, from the structure refinement data, the approximate gross composition of the studied single crystals as follows:

holotype udinaite *(1)* $(Na_{0.70}Ca_{0.1}\square_{0.15})Mg_4(V_{1.42}As_{1.30}P'_{0.28})O_{12}$

holotype arsenudinaite *(2)* $(Na_{0.70}Ca_{0.15}\square_{0.15})Mg_4(As_{1.64}V_{0.96}P'_{0.40})O_{12}$

arsenudinaite *(3)* $NaMg_4(As_{2.76}V_{0.12}P_{0.12})_{\sum 3.00}O_{12}$
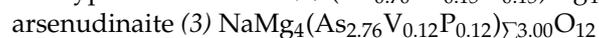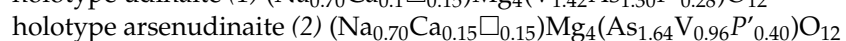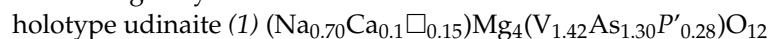
The main individual, species-defining feature to distinguish udinaite from arsenudinaite is the general prevailing of V or As in the mineral while the compositions of *M* and *A* cations are close in both minerals (Table 2). Ionic radii of V^{5+} and As^{5+} are close (0.355 and 0.335 Å, respectively, for tetrahedral coordination [14]) that causes the closeness of unit-cell dimensions and powder X-ray diffraction patterns of udinaite and arsenudinaite (Tables 1

and 3). At the same time, substitution of V^{5+} for As^{5+} results in the distinct increase in density and decrease in refractive indices of arsenudinaite in comparison with udinaite (Table 1). The latter effect is in general characteristic for pairs of isotypic vanadates and arsenates [15].

5.2. Comparative Crystal Chemistry

Udinaite and arsenudinaite represent the well-known synthetic compounds structure type of $NaMg_4(VO_4)_3$ [7], or $Mg_{0.5}Mg_4(AsO_4)_3 = Mg_3(AsO_4)_2$ [9]. This includes compounds with the general formula $^{VIII}A^{VI}M_4^{IV}T_3O_{12}$ (Roman numerals in formulae here and below mean coordination numbers) in which the dodecahedrally coordinated A site is filled by Na, Li, Mg, Mn^{2+}, Co^{2+}, Ni^{2+}, Fe^{2+}, Fe^{3+}, Y, Ca or partially vacant, the octahedrally coordinated M sites are occupied by Mg, Mn^{2+}, Co^{2+}, Ni^{2+}, Fe^{2+}, Fe^{3+} or Al and the tetrahedrally coordinated T sites are mainly filled by V^{5+}, As^{5+}, Ge^{4+}, Si or Fe^{3+}. All of these compounds have tetragonal symmetry, space group *I*-42*d*, close unit-cell dimensions, and similar powder XRD patterns [5–11,14–19].

Among them, only the phase with the simplified formula $(Mg,Fe)(Mg_{0.5}Al_{0.5})_4Si_3O_{12}$ was earlier known in nature, as inclusions in diamonds of lower-mantle origin. It was reported under a provisional name TAPP, "tetragonal almandine-pyrope phase" [20,21], and has the same chemical composition as an Fe-bearing pyrope; however, it strongly differs from garnets in terms of structure. TAPP was studied in detail in [22] and described, after the IMA approval as a mineral species (IMA2014-097) with the name jeffbenite and the idealized formula $Mg_3Al_2Si_3O_{12}$. The members of the udinaite–arsenudinaite isomorphous series are the second and third natural representatives of the $NaMg_4(VO_4)_3 = Mg_{0.5}Mg_4(AsO_4)_3$ = jeffbenite structure type. Later, niasite $Ni_{4.5}(AsO_4)_3 = Ni_{0.5}Ni_4(AsO_4)_3$ (IMA2019-105) with the same structure was discovered in the material from the abandoned mine at Johanngeorgenstadt, Saxony, Germany [23].

Besides representatives of the $^{VIII}Na^{VI}Mg_4(^{IV}VO_4)_3$ structure type, chemically different members of the garnet supergroup and arsenates and phosphates of the alluaudite supergroup demonstrate the same stoichiometry $Me_5(TO_4)_3$ ($Me = M + A$). All three structure types are strongly different. In particular, they show different ratios between the octahedrally coordinated M cations and the A cations with other coordination numbers. Oxysalt and oxide garnets (mainly cubic, *Ia*-3*d*) are characterized by the general formula $^{VIII}A_3^{VI}M_2^{IV}T_3O_{12}$ and the A cations centre oxygen dodecahedra [24]. Alluaudite-type compounds (monoclinic, *C*2/*c*) have the general formula $A(1)A(2)^{VI}M_3^{IV}T_3O_{12}$; the $A(1)$ cations have eight-, ten-, six- or even four-fold (flat square for Cu^{2+}) coordination, and the $A(2)$ cations centre eight- or six-fold polyhedra [25]. In the Arsenatnaya fumarole, we observe close association of arsenate and vanadate minerals with species-defining Mg (^{VI}M), Na and Ca (^{VIII}A) belonging to all three above-listed structure types with the same general stoichiometry: members of the continuous isomorphous series udinaite $NaMg_4(VO_4)_3$—arsenudinaite $NaMg_4(AsO_4)_3$ ($NaMg_4(VO_4)_3$ structure type, tetragonal, $M:A$ = 4:1), members of the continuous isomorphous series schäferite $(Ca_2Na)Mg_2(VO_4)_3$—berzeliite $(Ca_2Na)Mg_2(AsO_4)_3$ (garnet structure type, cubic, $M:A$ = 2:3) [26], calciojohillerite $NaCaMg_3(AsO_4)_3$ (alluaudite structure type, monoclinic, $M:A$ = 3:2) [27] and paraberzeliite $NaCa_2Mg_2(AsO_4)_3$ (alluaudite structure type, monoclinic, $M:A$ = 2:3) [28]. Crystal chemical features of the series udinaite–arsenudinaite and schäferite–berzeliite are similar here: wide isomorphism between V^{5+} and As^{5+} in tetrahedrally coordinated T sites and almost no admixtures in sites occupied by alkali-earth and alkali cations.

5.3. Notes on Genetic Features

Udinaite and arsenudinaite are fumarolic minerals formed at temperatures not lower than 470–500 °C. They were deposited directly from the gas phase as volcanic sublimates or, more probably, formed as a result of the interaction between fumarolic gas and basalt scoria. The latter could be a source of Mg and Ca, which have low volatility in fumarolic systems at temperatures up to 400–500 °C [29].

Unlike the orthosilicate jeffbenite, which crystallizes under high pressure and temperatures and was assumed as a pressure marker for detecting super-deep diamonds [22], the orthovanadate and orthoarsenate of this structure type, udinaite and arsenudinaite, were formed in the Arsenatnaya fumarole under atmospheric pressure and the suggested temperature interval 500–700 °C [3]. Similar conditions of formation can be suggested for niasite, probably a product of a high-temperature nickeline oxidation during the fire [23].

Probably, the combination of high temperature (>470–500 °C) and atmospheric pressure together with strong oxidizing conditions [2] favours wide isomorphism between high-valence (penta- and hexavalent) components in minerals crystallized in the hottest zones of the Arsenatnaya fumarole. Seven continuous isomorphous series/systems are found by us in this part of Arsenatnaya (pairs/triads of major variables are in parentheses): arsenudinaite–udinaite (As^{5+}–V^{5+}), berzeliite–schäferite (As^{5+}–V^{5+}), isokite–tilasite–reznitskyite (P^{5+}–As^{5+}–V^{5+}), fluorapatite–svabite–pliniusite (P^{5+}–As^{5+}–V^{5+}), wagnerite–arsenowagnerite (P^{5+}–As^{5+}), powellite–scheelite (Mo^{6+}–W^{6+}), and rhabdoborite-(V)–rhabdoborite-(Mo)–rhabdoborite-(W) (V^{5+}–Mo^{6+}–W^{6+}).

Author Contributions: Conceptualization, I.V.P. and N.N.K.; Methodology, I.V.P., N.N.K., N.V.Z., S.N.B., and D.Y.P.; Investigation, I.V.P., N.N.K., N.V.Z., D.I.B., M.F.V., A.A.A., D.A.K., A.G.T., S.N.B., and E.G.S.; Original Manuscript—Draft Preparation, I.V.P., N.N.K., and N.V.Z.; Manuscript—Review and Editing, I.V.P., N.N.K., S.N.B., and D.Y.P.; Figures, N.N.K., N.V.Z., and M.F.V. All authors have read and agreed to the published version of the manuscript.

Funding: The studies were supported by the Russian Science Foundation, grant no. 20-77-00063.

Data Availability Statement: The data presented in this study are available on request from the corresponding author.

Conflicts of Interest: The authors declare no conflict of interest.

References

1. Fedotov, S.A.; Markhinin, Y.K. (Eds.) *The Great Tolbachik Fissure Eruption*; Cambridge University Press: New York, NY, USA, 1983.
2. Pekov, I.V.; Koshlyakova, N.N.; Zubkova, N.V.; Lykova, I.S.; Britvin, S.N.; Yapaskurt, V.O.; Agakhanov, A.A.; Shchipalkina, N.V.; Turchkova, A.G.; Sidorov, E.G. Fumarolic Arsenates—A Special Type of Arsenic Mineralization. *Eur. J. Mineral.* **2018**, *30*, 305–322. [CrossRef]
3. Shchipalkina, N.V.; Pekov, I.V.; Koshlyakova, N.N.; Britvin, S.N.; Zubkova, N.V.; Varlamov, D.A.; Sidorov, E.G. Unusual Silicate Mineralization in Fumarolic Sublimates of the Tolbachik Volcano, Kamchatka, Russia—Part 1: Neso-, Cyclo-, Ino- And Phyllosilicates. *Eur. J. Mineral.* **2020**, *32*, 101–119. [CrossRef]
4. Britvin, S.N.; Dolivo-Dobrovolsky, D.V.; Krzhizhanovskaya, M.G. Software for Processing the X-Ray Powder Diffraction Data Obtained from the Curved Image Plate Detector of Rigaku RAXIS Rapid II Diffractometer. *Zap. Ross. Mineral. Obs.* **2017**, *146*, 104–107.
5. Nakamoto, K. *Infrared and Raman Spectra of Inorganic and Coordination Compounds*; John Wiley & Sons: New York, NY, USA, 1986.
6. Sheldrick, G.M. A Short History of SHELX. *Acta Crystallogr. Sect. A Found. Crystallogr.* **2008**, *64*, 112–122. [CrossRef] [PubMed]
7. Murashova, E.V.; Velikodnyi, Y.A.; Trunov, V.K. Crystal Structure of $NaMg_4(VO_4)_3$. *J. Struct. Chem.* **1988**, *29*, 648–650. [CrossRef]
8. Anissa, H.A.; Brahim, A.; Amor, H. $NaMg_4(AsO_4)_3$. *Acta Crystallogr. Sect. E Struct. Rep. Online* **2004**, *E60*, i77–i79. [CrossRef]
9. Krishnamachari, N.; Calvo, C. Magnesium Arsenate, $Mg_3As_2O_8$. *Acta Crystallogr. Sect. B Struct. Crystallogr. Cryst. Chem.* **1973**, *B29*, 2611–2613. [CrossRef]
10. Gopal, R.; Rutherford, J.S.; Robertson, B.E. Closest Packing in Dense Oxides: The Structure of a Polymorph of $Co_3(AsO_4)_2$. *J. Solid State Chem.* **1980**, *32*, 29–40. [CrossRef]
11. Barbier, J. IUCr Tetragonal $Ni_{4.35}As_3O_{11.7}(OH)_{0.3}$. *Acta Crystallogr. Sect. C* **1999**, *C55*, IUC9900080. [CrossRef]
12. Levy, D.; Barbier, J. $^{VIII}(Mg,Fe)_{0.85}^{VI}(Mg,Fe)_4^{IV}(Fe,Ge)_3O_{12}$: A New Tetragonal Phase and Its Comparison with Garnet. *Am. Mineral.* **2000**, *85*, 1053–1060. [CrossRef]
13. Clemens, O.; Haberkorn, R.; Beck, H.P. New Phases in the System $LiMnVO_4Mn_3(VO_4)_2$. *J. Solid State Chem.* **2011**, *184*, 2640–2647. [CrossRef]
14. Shannon, R.D. Revised Effective Ionic Radii and Systematic Studies of Interatomic Distances in Halides and Chalcogenides. *Acta Crystallogr. Sect. A* **1976**, *32*, 751–767. [CrossRef]
15. Fleischer, M.; Wilcox, R.E.; Matzko, J.J. *Microscopic Determination of Nonopaque Minerals*; US Geological Survey Bulletin: Washington, DC, USA, 1984.
16. Modaressi, A.; Gerardin, R.; Malaman, B.; Gleitzer, C. Structure et Propriétés d'un Germanate de Fer de Valence Mixte $Fe_4Ge_2O_9$. Etude Succincte de $Ge_xFe_{3−x}O_4$ (x ≤ 0.5). *J. Solid State Chem.* **1984**, *53*, 22–34. [CrossRef]

17. Tyutyunnik, A.P.; Zubkov, V.G.; Surat, L.L.; Slobodin, B.V. Synthesis and Crystal Structure of LiMg$_4$(VO$_4$)$_3$. *Russ. J. Inorg. Chem.* **2004**, *49*, 553–559.

18. Clemens, O.; Haberkorn, R.; Springborg, M.; Beck, H.P. Neutron and X-ray Diffraction Studies on the High Temperature Phase of Mn3(VO4)2, the New Isostructural Compound NaMn4(VO4)3 and Their Mixed Crystals NaxMn4.5−x/2(VO4) 3 (0≤ x≤ 1). *J. Solid State Chem.* **2012**, *194*, 409–415. [CrossRef]

19. Ben Yahia, H.; Gaudin, E.; Rodewald, U.C.; Pottgen, R. Synthesis and Structure of the Ternary Vanadate NaMn$_4$(VO$_4$)$_3$. *Zeitschrift Naturforsch. Sect. B J. Chem. Sci.* **2011**, *66*, 437–440. [CrossRef]

20. Harris, J.; Hutchison, M.T.; Hursthouse, M.; Light, M.; Harte, B. A New Tetragonal Silicate Mineral Occurring as Inclusions in Lower-Mantle Diamonds. *Nature* **1997**, *387*, 486–488. [CrossRef]

21. Finger, L.W.; Conrad, P.G. The Crystal Structure of "Tetragonal Almandine-Pyrope Phase" (TAPP): A Reexamination. *Am. Mineral.* **2000**, *85*, 1804–1807. [CrossRef]

22. Nestola, F.; Burnham, A.D.; Peruzzo, L.; Tauro, L.; Alvaro, M.; Walter, M.J.; Gunter, M.; Anzolini, C.; Kohn, S.C. Tetragonal Almandine-Pyrope Phase, TAPP: Finally a Name for It, the New Mineral Jeffbenite. *Mineral. Mag.* **2016**, *80*, 1219–1232. [CrossRef]

23. Kampf, A.R.; Nash, B.P.; Plášil, J.; Smith, J.B.; Feinglos, M.N. Niasite and Johanngeorgenstadtite, Ni$^{2+}_{4.5}$(AsO$_4$)$_3$ Dimorphs from Johanngeorgenstadt, Germany. *Eur. J. Mineral.* **2020**, *32*, 373–385. [CrossRef]

24. Grew, E.S.; Locock, A.J.; Mills, S.J.; Galuskina, I.O.; Galuskin, E.V.; Hålenius, U. Nomenclature of the Garnet Supergroup. *Am. Mineral.* **2013**, *98*, 785–811. [CrossRef]

25. Hatert, F. A New Nomenclature Scheme for the Alluaudite Supergroup. *Eur. J. Mineral.* **2019**, *31*, 807–822. [CrossRef]

26. Koshlyakova, N.N.; Pekov, I.V.; Zubkova, N.V.; Agakhanov, A.A.; Turchkova, A.G.; Kartashov, P.M.; Sidorov, E.G.; Pushcharovsky, D.Y. A New Solid Solution with Garnet Structure: Berzeliite–Schäferite Isomorphic Series from the Fumarole Exhalation of the Tolbachik Volcano, Kamchatka. *Geol. Ore Depos.* **2021**, *63*, 857–868. [CrossRef]

27. Pekov, I.V.; Koshlyakova, N.N.; Agakhanov, A.A.; Zubkova, N.V.; Belakovskiy, D.I.; Vigasina, M.F.; Turchkova, A.G.; Sidorov, E.G.; Pushcharovsky, D.Y. New Arsenate Minerals from the Arsenatnaya Fumarole, Tolbachik Volcano, Kamchatka, Russia. XV. Calciojohillerite, NaCaMgMg$_2$(AsO$_4$)$_3$, a Member of the Alluaudite Group. *Mineral. Mag.* **2021**, *85*, 215–223. [CrossRef]

28. Pekov, I.V.; Koshlyakova, N.N.; Belakovskiy, D.I.; Vigasina, M.F.; Zubkova, N.V.; Agakhanov, A.A.; Britvin, S.N.; Sidorov, E.G.; Pushcharovsky, D.Y. New Arsenate Minerals from the Arsenatnaya Fumarole, Tolbachik Volcano, Kamchatka, Russia. XVII. Paraberzeliite, NaCaCaMg$_2$(AsO$_4$)$_3$, an Alluaudite-Group Member Dimorphous with Berzeliite. *Mineral. Mag.* **2022**, *86*, 103–111. [CrossRef]

29. Symonds, R.B.; Reed, M.H. Calculation of Multicomponent Chemical Equilibria in Gas-Solid-Liquid Systems; Calculation Methods, Thermochemical Data, and Applications to Studies of High-Temperature Volcanic Gases with Examples from Mount St. Helens. *Am. J. Sci.* **1993**, *293*, 758–864. [CrossRef]